Journal of Molecular Liquids 342 (2021) 117464

Contents lists available at ScienceDirect

Journal of Molecular Liquids

journal homepage: www.elsevier.com/locate/molliq

On the important transition of sugar-based surfactant as a microreactor for C-S coupling in water: From micelle to vesicle

Xin Ge [a,*], Qiuyun Lei [a], Siyuan Wu [a], Xiong Liao [a], Weili Song [a], Lei Wu [b], Xuemin Liu [a], Shaodong Zhou [b,*]

[a] School of Chemical and Material Engineering, Jiangnan University, Wuxi, PR China
[b] Zhejiang Provincial Key Laboratory of Advanced Chemical Engineering Manufacture Technology, College of Chemical and Biological Engineering, Zhejiang University, Hangzhou, PR China

ARTICLE INFO

Article history:
Received 2 May 2021
Revised 4 August 2021
Accepted 1 September 2021
Available online 8 September 2021

Keywords:
Vesicular catalysis
In water
C-S Coupling
Sugar-based Surfactant

ABSTRACT

A reversible, temperature-induced micelle-to-vesicle transition of a sugar-based pseudogemini surfactant ($C_{11}D_{12}$) was employed for copper-catalyzed C-S coupling in water. The phase behavior and morphology of the $C_{11}D_{12}$ aqueous solution were investigated by DLS and cryo-TEM. The aggregates undergo a series of transitions upon increasing the temperature: spherical micelles were initially transformed into large vesicles, but they eventually transformed into smaller vesicles. The vesicular catalytic protocol accommodates an excellent substrate scope with moderate to high yields. The mechanisms of temperature-induced aggregate transition and vesicular catalysis were elucidated by experimental results and DFT calculations. It was revealed that the charge layer of the vesicle grants stronger nucleophilicity to the $PhSO_2$-Cu-D_{12}Ga intermediate. Furthermore, the aqueous reaction medium can be recycled and reused several times after easily separating the precipitated product.

1. Introduction

Sulfones are important structural motifs that are widely used in natural products [1] and clinical drugs [2–4]. Recently, the metal-catalyzed coupling of sulfonate salts with aryl halides has emerged into the spotlight of chemical research [5–9]. Challenges to this approach include the choice of appropriate ligands and the use of eco-friendly media. Green protocols that avoid using hazardous organic solvents continue to be demanding. Surfactant-mediated aqueous organic reactions are known for their self-assembly properties, generating micelles or other organized aggregates in aqueous solutions [10]. Micellar catalysis continues to attract significant attention due to the ideal solubility of hydrophobic substances in micelles, which can serve as nanoreactors for organic reactions [11–14]. Therefore, a series of commercially available surfactant-based aggerates such as SDS [15], CTAB [16], Brij-35 [17], Triton X-100 [18], and Tween 20/40 [19] have been employed for implementing organic transformations. However, these commercial surfactants cannot meet the needs of various organic reactions. A significant amount of effort has been made by many groups, including those of Lipshutz and Handa, to explore powerful and versatile surfactants such as PTS [20,21], TPGS-750-M [22-26], NOK [27,28], and FI-750-M [24,29-33] for performing various organic reactions in water. These newly designed surfactants were constructed by modifying the structure of amphiphiles, e.g., the length of the hydrophobic chain and regulation of the core group, to comply with the "like dissolves like" rule. With the exception of the wormlike micelles of NOK, most of the newly designed surfactants form spherical micelles with aggregate sizes of 10–100 nm [11]. In particular, TPGS-750-M, with a diameter of 53–65 nm, preferentially accommodates all exchanging ingredients to allow the desired reaction to take place [34]. Thus, a coupling reaction with TPGS-750-M was more efficient than with PTS, which has an average micellar size of 22 nm. Similarly, PiNap-750 M exhibited higher catalytic activity than BTBT-750 M due to its larger micellar size [35]. Therefore, the morphology of aggregates, including size and shape, is crucial for achieving desired chemical transformations.

Micellar catalysis is inspired by nature and intrinsically mimics cell membranes that allow transformations in aqueous environment [36]. Although micelles are similar to cell membranes, liposomes made of cell membranes are phospholipid vesicles, an aggregate type different than micelles [37]. Vesicles are usually comprised of double-chain amphiphiles. Until now, mixing cationic and anionic single surfactants has been one of the most convenient and efficient approaches for forming vesicles [38]. In 2005, Engberts *et al.* studied nucleophilic substitution of aromatic alkylsulfonates with bromide ions and water in the presence of vesicles

* Corresponding authors.
E-mail addresses: gexin@jiangnan.edu.cn (X. Ge), szhou@zju.edu.cn (S. Zhou).

https://doi.org/10.1016/j.molliq.2021.117464
0167-7322/

composed of 1-palmitoyl-2-oleoyl-*sn*-glycero-3-phosphocholine, di-*n*-hexadecyldimethylammonium bromide, and *n*-dodecyl-*β*-glucoside [39]. In 2016, Movahedi *et al.* reported an Fe-cysteine biocatalyst in a vesicular aqueous solution in which sodium dodecyl sulfate and dodecyltrimethylammonium bromide (SDS/DTAB) were mixed [40]. Nevertheless, compared with micellar catalysis, vesicular catalysis in water has received less attention [41,42]. Moreover, although ionic surfactants can be induced to enable the spontaneous formation of vesicles, such surfactant systems are generally complicated. In 2017, we reported a temperature-induced micelle-to-vesicle transition with a single pseudogemini surfactant [43]. However, it is still unknown whether it is possible to develop a vesicular catalytic system in water by aggregate transition in a single surfactant aqueous solution.

Sugar, composed of polyhydric hydrophilic structures, can be attached to a hydrophobic chain to produce a surface-active substance [44,45]. Due to their eco-friendliness, renewable nature, and biodegradable characteristics, sugar-based surfactants have attracted significant attention and play an important role in cosmetics, pharmaceuticals, biochemistry, and gene transfection [46-50]. Recently, a series of novel sugar-based surfactants were designed and synthesized [45,51-59]. Interestingly, a transition of aggregates was not observed in these sugar-based surfactants [51,60-62]. In our previous work [63], pseudogemini surfactants were constructed using *N*-dodecyl glucosamine (and *N*-dodecyl lactosamine) and dicarboxylic acid ($HOOC(CH_2)_{n-2}COOH$, n = 3, 4, 5, 6, 8) in aqueous solution via non-covalent bonds. The influence of spacer group length on their physicochemical properties was studied without the occurrence of coacervation. In this work, a micelle-to-vesicle transition was observed in an aqueous solution of a sugar-based pseudogemini surfactant ($C_{11}D_{12}$, Fig. 1) non-covalently constructed with *N*-dodecylglucosamine ($D_{12}Ga$) and undecanedioic acid. The size and morphology of aggregate transition was studied by changing the temperature. Furthermore, the aggregates generated by $C_{11}D_{12}$ were applied in a copper-catalyzed C-S coupling reaction in water, exhibiting superb catalytic performance.

2. Results and discussion

2.1. Aggregate transition in $C_{11}D_{12}$ aqueous solution

Critical micelle concentration (CMC) is an important characteristic of surfactants [64-66]. As shown in Fig. S1, the CMC value of the sugar-based pseudogemini surfactant $C_{11}D_{12}$ was determined to be 0.56 mM. The surface tension decreases sharply when increasing the concentration of $C_{11}D_{12}$ aqueous solution until a break point appears. Furthermore, above the CMC, the value of the surface tension is almost constant. It is clear that the sugar-based pseudogemini surfactant $C_{11}D_{12}$ was successfully synthesized by the *in-situ* neutralization reaction of *N*-dodecyl glucosylamine and undecanedioic acid in water. To investigate the aggregation of the surfactant in aqueous solution, the conductivities of $C_{11}D_{12}$ at different temperatures (25 °C, 35 °C, 45 °C, and 55 °C) were examined. The specific calculation formula is based on a previously reported method [67] and the results are shown in Fig. 2 and Table 1. The CMC was obtained by conductivity method at 25 °C. The ΔG_m^0 value of $C_{11}D_{12}$ is negative at 25–55 °C. Therefore, the formation of $C_{11}D_{12}$ micelles is a thermodynamic spontaneous process. In addition, the negative value of ΔH_m^0 indicates that the micellization process is exothermic. The value of $T\Delta S_m^0$ is greater than the absolute value of ΔH_m^0, which indicates that the micellization process is entropy-driven. Taking these data into account, the micellization of $C_{11}D_{12}$ is a thermodynamic, spontaneous, and exothermic process.

The phase behavior of the $C_{11}D_{12}$ aqueous solution was studied at a fixed concentration of 1 mM. The turbidity of the $C_{11}D_{12}$ aqueous solution was determined by the absorbance at 600 nm using a UV–vis spectrophotometer (UV-2700). The break point in the absorbance was determined to be 41.2 °C, indicating that aggregate transition takes place at this temperature. The effect of temperature on the aggregates of the 1 mM $C_{11}D_{12}$ aqueous solution was examined and the results are summarized in Fig. 3. When the temperature was controlled at 39 °C, the average diameter of aggregates in the homogenous and transparent solution was 8.5 nm. When the temperature was increased to 40 °C, aggregates with a diameter of 263.6 nm were gradually formed and the solution turned pale blue, a characteristic feature of solutions containing vesicles. Increasing the temperature to 45 °C resulted in the disappearance of 8.2 nm aggregates, and only 113.4 nm diameter aggregates were formed. At this temperature, the solution became cloudy and turbid. These results provide preliminary evidence for a micelle-to-vesicle transition. Moreover, the temperature of the break point is defined as the temperature of self-assembly transition from micelle to vesicle (T_{MVT}). To further elucidate the microstructures of the 1 mM $C_{11}D_{12}$ aqueous solution at 39 °C and 45 °C, the morphology of the aggregates was studied by cryo-TEM (Fig. 3c, d). The aggregates at 39 °C are spherical micelles with an average diameter of 8.5 nm, while at 45 °C, vesicles with an average diameter of 122.8 nm are present. This verifies that the transition of aggregates from spherical micelles to vesicles is induced by increasing the temperature. Moreover, further increasing temperature causes a decrease in vesicle size. The vesicles at 100 °C are about 24 nm in diameter and 4 nm in wall thickness,

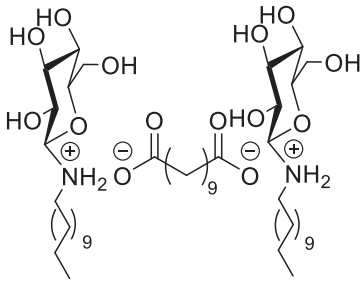

Fig. 1. Chemical structure of sugar-based pseudogemini surfactant ($C_{11}D_{12}$).

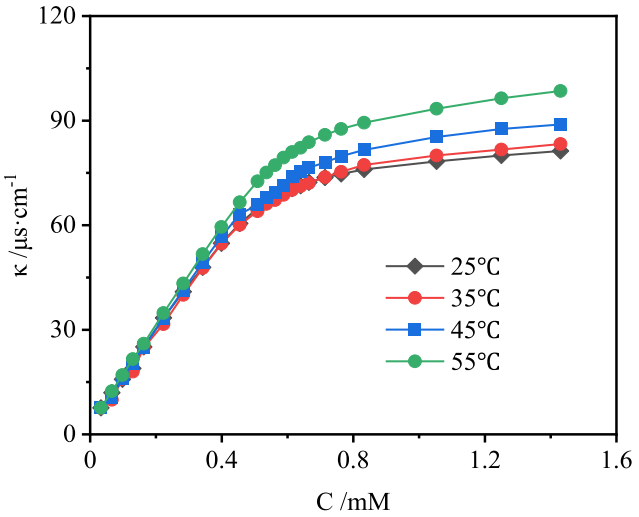

Fig. 2. Dependence of the electroconductivity (κ) of $C_{11}D_{12}$ aqueous solution on surfactant concentration (*c*) at different temperatures.

Table 1
Thermodynamic parameters of $C_{11}D_{12}$.

Surfactant	T/°C	CMC/mM	β	ΔG_m^0/KJ·mol^{-1}	ΔH_m^0/KJ·mol^{-1}	$T\Delta S_m^0$/KJ·mol^{-1}
$C_{11}D_{12}$	25	0.582	0.894	−40.49	−1.892	38.60
	35	0.605	0.872	−41.07	−1.989	39.08
	45	0.607	0.859	−41.99	−2.100	39.89
	55	0.618	0.852	−43.03	−2.223	40.81

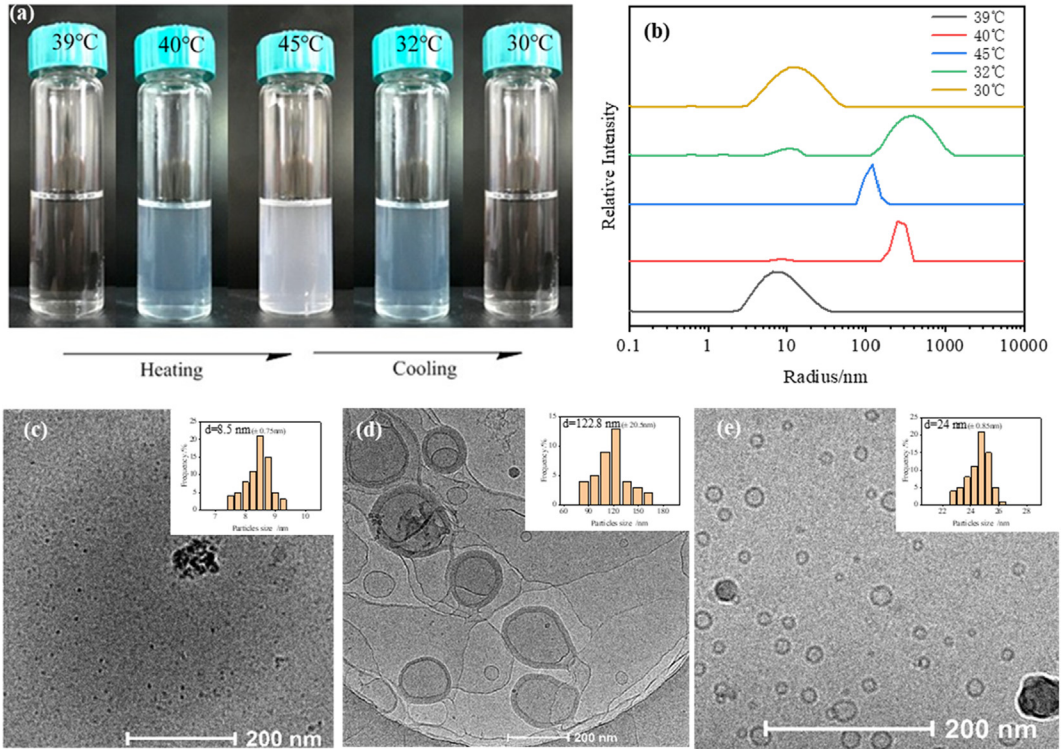

Fig. 3. Effect of temperature on aggregates of 1 mM $C_{11}D_{12}$ aqueous solution: (a) image of solutions at different temperatures, (b) DLS results for aggregate size distribution, and (c, d, e) cryo-TEM images at 39 °C, 45 °C, and 100 °C (insets: particle size distribution).

and they have good dispersibility in aqueous solution. In contrast, decreasing the temperature reversed the turbidity phenomena. When the temperature was dropped to 32 °C, the average diameters of the two types of aggregate were 10.0 nm and 380.5 nm, respectively, causing the solution to become pale blue. Finally, at 30 °C, the solution returned to a clear and transparent state with an aggregate size of about 10 nm. Furthermore, this turbidity phenomenon was able to be reversed at least 20 times. The micelle-to-vesicle transition solution was generally homogenous, but occasionally became cloudy, eventually forming an aqueous two-phase system (ATPS). Above the T_{MVT}, the $C_{11}D_{12}$ aqueous solution becomes an ATPS after reaching thermodynamic equilibrium (12 h), exhibiting a clear phase boundary in Fig. S3. Furthermore, the T_{MVT} curve of the $C_{11}D_{12}$ aqueous solution is illustrated in Fig. 4. It is clear that T_{MVT} decreases when the concentration of the $C_{11}D_{12}$ aqueous solution is increased. The region below the T_{MVT} curve is homogenous, whereas ATPS is located above the T_{MVT} curve.

The mechanism of temperature-driven micelle-to-vesicle transition of the $C_{11}D_{12}$ aqueous solution is proposed based on the variation of components involved in the aggregates. $C_{11}D_{12}$ non-covalently constructed by *N*-dodecylglucosamine and undecanedioic acid is a sugar-based pseudogemini surfactant formed by the strong attraction between oppositely charged hydrophilic spacers and hydrophobic tails. As shown in Fig. 5, $C_{11}D_{12}$ in water

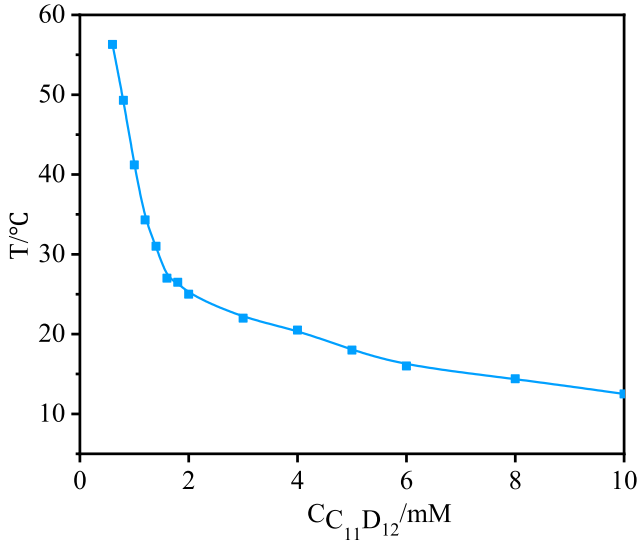

Fig. 4. Variation of T_{MVT} with the concentration of $C_{11}D_{12}$ in aqueous solution.

initially self-assembles to form a micelle. Because electrostatic attraction is a weaker physical force compared with covalent

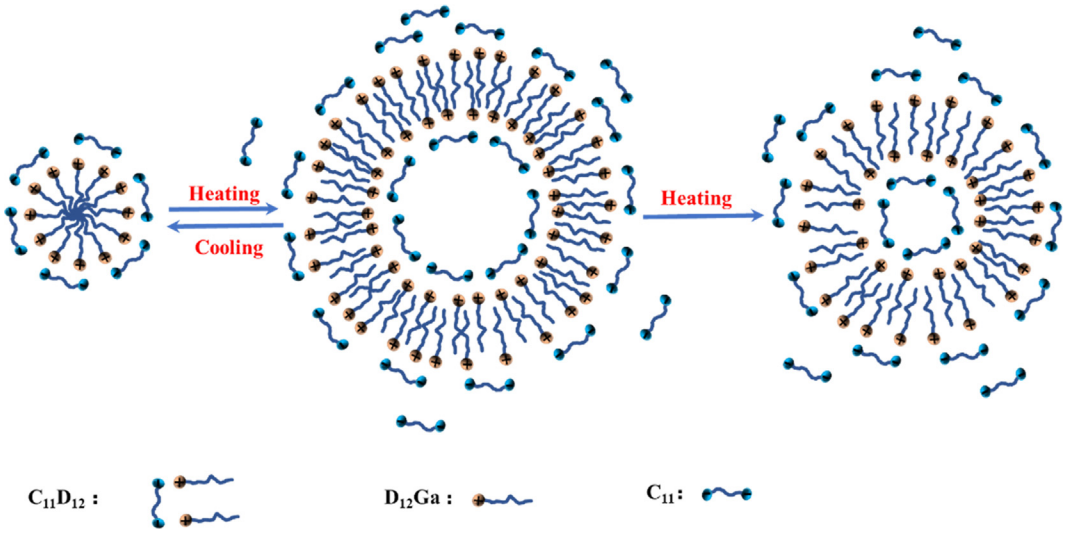

Fig. 5. Mechanism of temperature-induced aggregate transition.

bonds, a higher temperature benefits the dissociation of the surfactant ion pairs. This causes an increase in the amount of free undecanedioic acid. This free undecanedioic acid dissolves from the aggregated form to the bulk aqueous solution, lowering the charge density of the micelle surface. On the other hand, *N*-dodecylglucosamine tends to solubilize in the palisade layer of the aggregates, resulting in an increase of hydrophobic tails and the formation of a positively charged surface. This was verified by measuring surface charge density. As shown in Fig. S4, the zeta potential of 1 mM $C_{11}D_{12}$ aqueous solution at 70 °C was measured to be 19.26 mV. The positive zeta potential value reveals that the surface of the vesicles is positively charged. Therefore, the micelles are forced to transform into other aggregates of lower curvatures, likely vesicles. Furthermore, the CP phenomenon is relevant for rapid aggregate transition from small micelles into large vesicles. Further raising the temperature allows thermally induced changes in the hydrophobic tails, increasing the fluidity of the tail groups [68]. Driven by the increase in curvature, the transition from large to small vesicles is induced.

2.2. Performance of vesicular catalysis for C-S coupling reaction in water

The copper-catalyzed synthesis of sulfones from sulfinate salts and aryl halides continues to attract significant attention in the medical industry [6,7]. Thus, the aggerates generated by surfactants were applied in a copper-catalyzed C-S coupling reaction in water. The cross-coupling of bromobenzene with sodium benzenesulfinate was selected as the model reaction, and the results are summarized in Table 1. Initially, a serial of commercially available surfactants including CTAB, SDS, Tween 20, Tween 60, Tween 80, Span 20, and newly designed surfactants including TPGS-750-M, $D_{12}Ga$, C_4D_{12}, C_8D_{12}, and $C_{11}D_{12}$ were evaluated (Table 2, entries 1–12). The catalytic performance in $C_{11}D_{12}$ aqueous solution is superior to that in $D_{12}Ga$, C_4D_{12}, C_8D_{12}, TPGS-750-M and the commercial surfactant aqueous solutions. In our previous work, micelles were formed in $D_{12}Ga$, C_4D_{12}, and C_8D_{12} aqueous solutions [44,63], whereas the aggregates in the $C_{11}D_{12}$ aqueous solution at 100 °C are vesicles. We speculate that these cationic vesicles can significantly promote the yield of the desired product. Furthermore, a control experiment showed that a surfactant is necessary for C-S coupling reactions in water. The optimal concentration of $C_{11}D_{12}$ in aqueous solution was found to be 1 mM (Table 2, entries 12–14). A comparison of various copper sources including CuI, CuBr, CuCl, $Cu(CH_3COO)_2$, $CuCl_2$, and $CuSO_4$ showed that CuBr was the best copper source (Table 2, entries 11, 15–19). Finally, different temperatures (70, 80, 90, and 100 °C) were examined (Table 2, entries 11, 20–22). A low temperature (70 °C) resulted in poor catalytic activity, and it was determined that 100 °C was the most suitable temperature.

With the optimized conditions, the scope of the copper-catalyzed C-S coupling process in $C_{11}D_{12}$ aqueous solution was examined (Table 3). Unlike a previous study, the reactivity of aryl bromide in this system is close to that of aryl iodine. To our disappointment, aryl chloride is still a poor substrate which did not obtain the desired product. The expected C-S coupling products **3** were obtained with excellent yields by using aryl bromide with electron donating groups such as 4-Me and 4-OMe. In contrast, electron withdrawing groups such as 4-Cl, 4-Ac, 4-NO_2, 3-NO_2, 4-CF_3 and 4-COOH were located in the aryl ring of bromobenzene and afforded corresponding product yields of 42–90%. Moreover, 4-bromobenzoic acid is less soluable in the lipophilic part due to its stronger polarity compared to other substrates with electron withdrawing groups, resulting in lowest yield. The yield slightly decreased with 2-halogenated pyridines, induced by the electronegative nitrogen in the pyridine ring. The steric hindrance from *ortho*-substituents had a significant influence on the reaction, and aryl bromide with a 2-Me group was converted into the final product with a 55% yield. Alkyl halides such as benzyl, *n*-octyl, and *n*-hexadecyl were converted into the desired sulfone with low yields due to their hydrolysis in water caused by high vesicular catalytic activity. Sodium arylsulfinates with 4-Me, 4-F, and 4-Cl groups afforded the corresponding products in good to excellent yields under the optimized reaction conditions. Furthermore, when the C-S coupling reaction was performed using sodium methyl, ethyl, and cyclopropyl sulfinates, the desired products were obtained in moderate yields. Finally, as a meaningful application of surfactant-mediated catalytic technology in water, the sulfone was synthesized in gram quantities by the catalysis of bromobenzene and sodium benzenesulfinate in $C_{11}D_{12}$ vesicular aqueous solution with an isolated final product yield of 90.5% (Scheme 1).

To further explore the vesicular catalytic mechanism, *in-situ* IR was used to monitor the interaction between $C_{11}D_{12}$ and CuBr (Fig. 6). When CuBr was added to the 1 mM $C_{11}D_{12}$ aqueous solution at 100 °C, the characteristic absorption peaks at 1563 cm^{-1}, 1544 cm^{-1} (N—H deformation vibration), and 1421 cm^{-1} (O—H

Table 2
Optimization of Ullmann C-S coupling in water.[a]

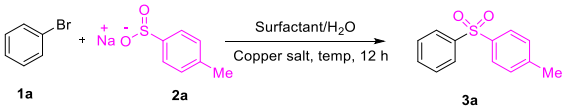

1a 2a 3a

Entry	Surfactant	Copper salt	Temp/℃	Yield/% [d]
1	–	CuBr	100	trace
2	CTAB	CuBr	100	8
3	SDS	CuBr	100	23
4	Tween 20	CuBr	100	28
5	Tween 60	CuBr	100	30
6	Tween 80	CuBr	100	29
7	Span-20	CuBr	100	9
8	TPGS-750-M	CuBr	100	72
9	$D_{12}Ga$	CuBr	100	80
10	C_4D_{12}	CuBr	100	65
11	C_8D_{12}	CuBr	100	75
12	$C_{11}D_{12}$	CuBr	100	95
13	$C_{11}D_{12}$ [b]	CuBr	100	70
14	$C_{11}D_{12}$ [c]	CuBr	100	80
15	$C_{11}D_{12}$	CuI	100	87
16	$C_{11}D_{12}$	CuCl	100	85
17	$C_{11}D_{12}$	$Cu(CH_3COO)_2$	100	70
18	$C_{11}D_{12}$	$CuCl_2$	100	55
19	$C_{11}D_{12}$	$CuSO_4$	100	65
20	$C_{11}D_{12}$	CuBr	90	85
21	$C_{11}D_{12}$	CuBr	80	80
22	$C_{11}D_{12}$	CuBr	70	trace

[a] Reaction conditions: bromobenzene (1.0 mmol), sodium benzenesulfinate (1.2 mmol), copper salt (0.1 mmol), 0.01 mmol surfactant in 10 mL water, 12 h.
[b] 0.005 mmol surfactant in 10 mL water.
[c] 0.02 mmol surfactant in 10 mL water.
[d] Isolated yield.

Table 3
Substrate scope of C-S couplings in $C_{11}D_{12}$ aqueous solution.[a]

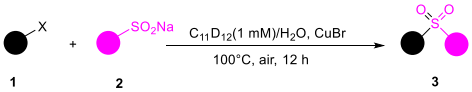

1 2 3

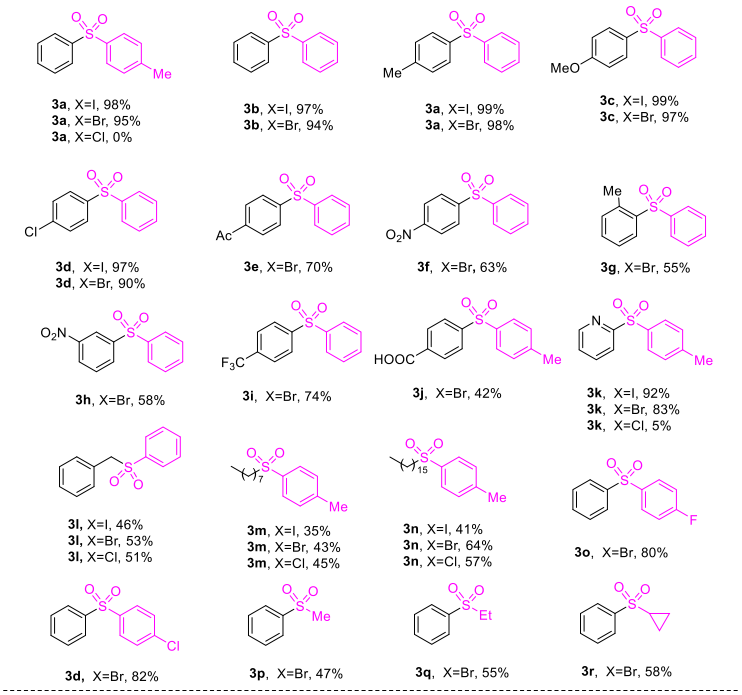

[a] Reaction Conditions: substrate **1** (1.0 mmol), substrate **2** (1.2 mmol), CuBr (0.1 mmol), and $C_{11}D_{12}$ (0.01 mmol) in water (10 mL) under air at 100 °C for 12 h. Isolated yield.

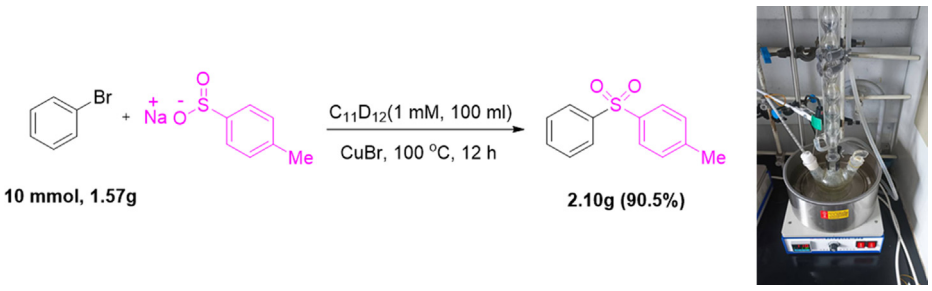

Scheme 1. Gram-scale synthesis of sulfone in $C_{11}D_{12}$ vesicular aqueous solution.

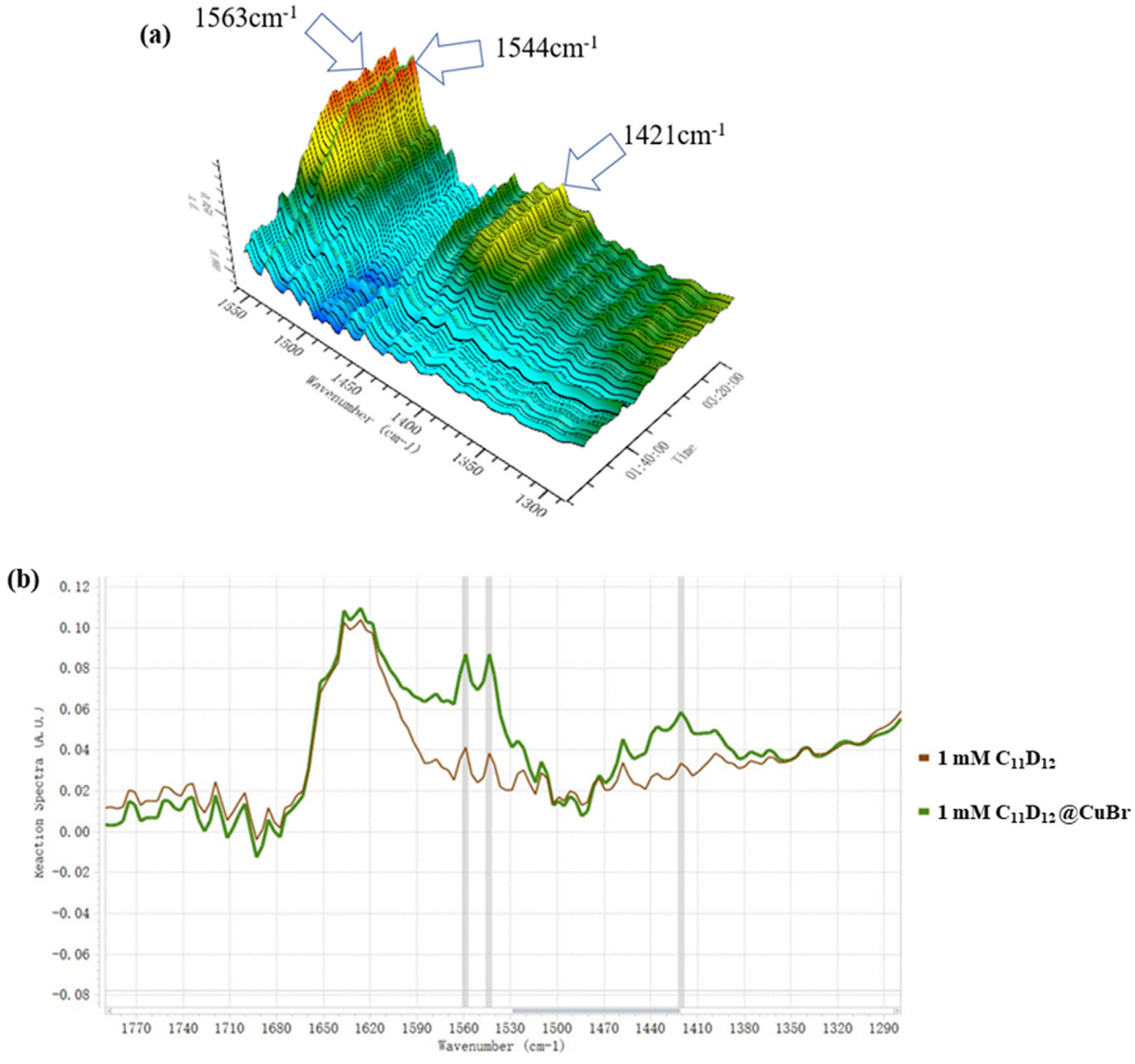

Fig. 6. CuBr added to 1 mM $C_{11}D_{12}$ aqueous solution: (a) overall three-dimensional Fourier transform IR (3D-FTIR) profile, (b) *in-situ* ConcIRT spectra.

bending vibration) became stronger. This implies that CuBr interacts with the surfactant $C_{11}D_{12}$ by the chelation of hydrophilic glycosyl and amino groups. In order to verify the encapsulation and aggregation of the substrates in vesicular aqueous solution, the vesicular size of the 1 mM $C_{11}D_{12}$ aqueous solution was measured by DLS. However, due to the 100 °C temperature exceeding the upper limit of the instrument, the temperature was set at 60 °C. As shown in Fig. S2, the vesicular size of the 1 mM $C_{11}D_{12}$ aqueous solution increased from 48 nm to 56 nm after dissolving bromobenzene (0.1 M) in the solution. This phenomenon indicates that the vesicles play a certain role in the encapsulation and aggregation of the substrate in water. Therefore, $C_{11}D_{12}$ in aqueous solu-

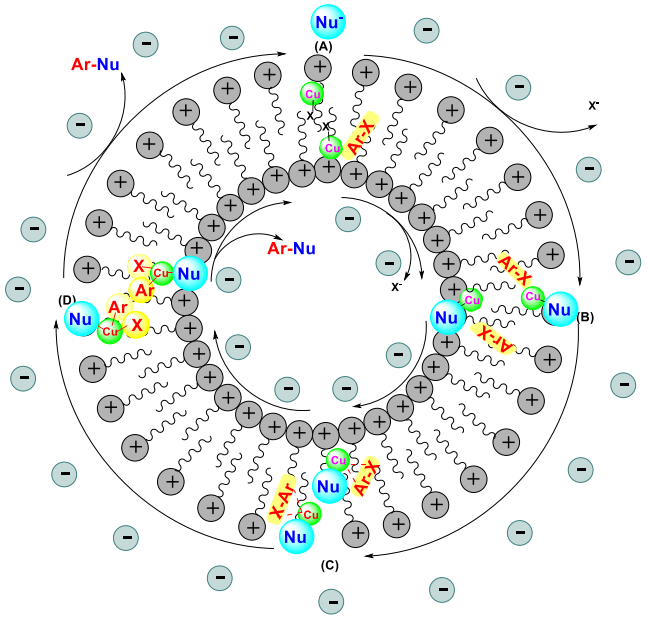

Fig. 7. Proposed reaction mechanism.

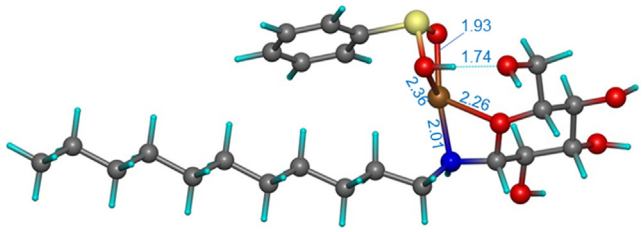

Fig. 8. Selected structural information of the $PhSO_2$-Cu-$D_{12}Ga$ molecule. When the $PhSO_2$-Cu unit approaches the $D_{12}Ga$ moiety, a hydrogen is spontaneously transferred from the latter to the former.

tion both provides a vesicle environment for the aggregation of substratesczz and potentially acts as a ligand to chelate the copper catalyst. Based on these experiments and previous reports [44], a plausible mechanism of vesicular catalysis for the copper-catalyzed C-S coupling reaction can be proposed. As shown in Fig. 7, vesicles with a positive surface charge are formed in 1 mM $C_{11}D_{12}$ aqueous solution at 100 °C. When CuBr is added into the solution, the hydrophilic glycosyl and amino groups of the surfactant enable the formation of metallic vesicles by chelating copper. Aryl bromides are concentrated in the bilayer of the vesicles, while arylsulfinates accumulate on the surface of the vesicles due to electrostatic interactions. Thus, the reaction occurs on the surface of the vesicular bilayer. Initially, the nucleophilic reaction of Cu-$D_{12}Ga$ with arylsulfinates generates a $PhSO_2$-Cu-$D_{12}Ga$ complex. A nucleophilic attack of the C-Br bond then prevails for the Cu-catalyzed C-S coupling of arylsulfinate sodium and aryl bromide. Finally, the desired product is obtained by reduction elimination with metallic vesicle regeneration.

Thus, the reactivity of the $PhSO_2$-Cu-$D_{12}Ga$ complex is important for the C—S coupling reaction. Based on infrared analysis, an optimized structure shown in Fig. 8 can be assumed to be the species directly reacting with the aryl bromide. Geometry optimization was performed at the GFN-xTB2 level using the xTB program, version 6.3.1 [69]. Orbital analysis was performed at the PBE0 [70]/def2-SV(P) [71] level using Gaussian 16, Revision A.03 [72]. As shown in Fig. 9a, (orbit 143) is the Cu-involved, highest occupied molecular orbital (HOMO), while (orbit 146) in Fig. 9b is the Cu-involved, lowest unoccupied molecular orbital (LUMO).

Furthermore, to explore the effect of electric field on the reactivity of benzenesulfinate, the influence of a point charge located near the benzenesulfinate molecule on the Cu-HOMO and Cu-LUMO was examined computationally. When the negative point charge gradually approaches Cu, the energies of Cu-HOMO and Cu-LUMO significantly increase (Fig. 10). A higher HOMO energy means stronger nucleophilicity, making the $PhSO_2$-Cu-$D_{12}Ga$ species more reactive with aryl bromide via nucleophilic attack of the C—Br bond. Therefore, it was verified that cationic vesicles can improve the catalytic efficiency for the C—S coupling reaction.

The reusability of the $C_{11}D_{12}$ vesicular catalyst was also studied based on the optimized conditions. When the reaction was complete and cooled down, the desired product precipitated as a white solid (Fig. S5) and a copper content of 59 ppm was detected by ICP-OES analysis. After easily separating the final product, the $C_{11}D_{12}$ aqueous solution system was recycled and directly reused. As

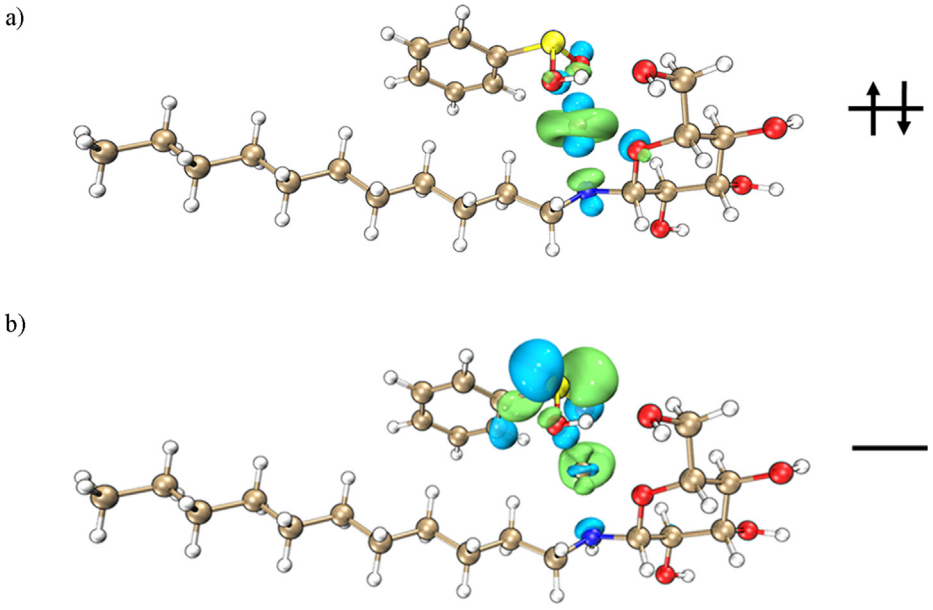

Fig. 9. (a) The HOMO of Cu. (b) The LUMO of Cu. (This figure was made using Multiwfn [73] and VMD [74]).

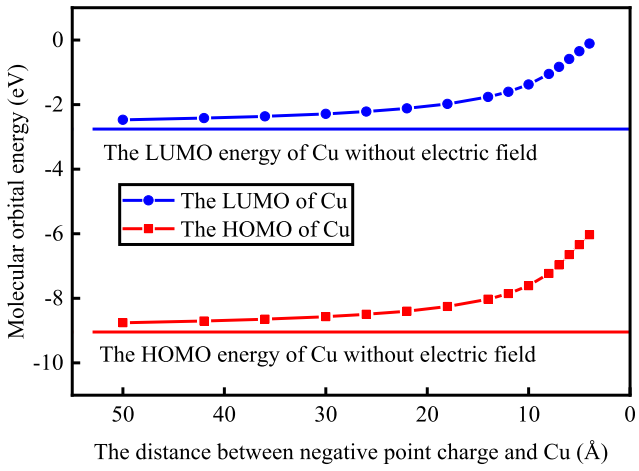

Fig. 10. The relationship of Cu-HOMO and Cu-LUMO energies with the distance between the negative point charge and Cu.

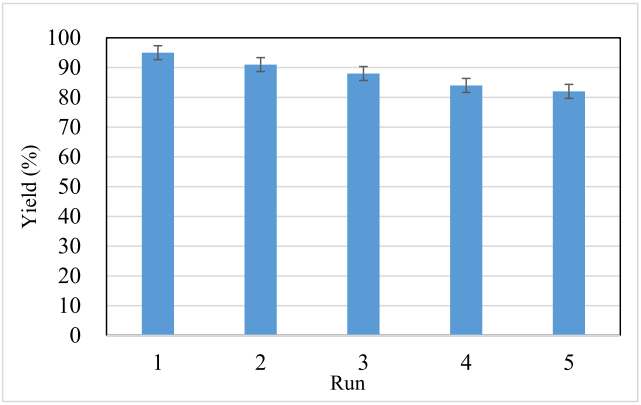

Fig. 11. Recycling and reuse of $C_{11}D_{12}$ aqueous solution.

shown in Fig. 11, the $C_{11}D_{12}$ aqueous solution could be reused five times with a small loss of activity that is potentially caused by a slight decrease in $C_{11}D_{12}$ surfactant concentration. However, it is clear that the surfactant aqueous system still exhibits good performance for the C—S coupling reaction after five runs.

3. Conclusion

In summary, we have investigated the aggregate transition of a sugar-based pseudogemini surfactant ($C_{11}D_{12}$) constructed by mixing *N*-dodecylglucosamine and undecanedioic acid in aqueous solution by adjusting the temperature. The physicochemical properties of $C_{11}D_{12}$ were studied by surface tension measurements and conductivity measurements. The reversible phase behavior and morphology were clarified by DLS and cryo-TEM. Spherical micelles with an average diameter of 8.5 nm at 39 °C were transformed into vesicles with an average diameter of 122.8 nm at 45 °C. When further increasing the temperature to 100 °C, the vesicles shrank to 24 nm in diameter and 4 nm in wall thickness. These cationic $C_{11}D_{12}$ vesicles can be used as a microreactor to efficiently promote a copper-catalyzed C—S coupling reaction in water. This vesicular catalytic protocol has an excellent substrate scope and affords the desired product in moderate to high yields. Notably, the $C_{11}D_{12}$ aqueous solution can be recycled and reused five times with satisfactory yield after separating the precipitated product. The vesicular catalytic mechanisms were elucidated by *in-situ* IR and theoretical calculations. It was revealed that the charge layer of the vesicles afforded stronger nucleophilicity of the $PhSO_2$-Cu-D_{12}Ga intermediate via an external electric field, making it more reactive with aryl bromide via nucleophilic attack of the C-Br bond.

CRediT authorship contribution statement

Xin Ge: Conceptualization, Methodology, Investigation, Data curation, Writing – original draft, Supervision. **Qiuyun Lei:** Methodology, Investigation, Data curation. **Siyuan Wu:** Investigation, Data curation. **Xiong Liao:** Methodology, Investigation. **Weili Song:** Methodology, Investigation. **Lei Wu:** Investigation. **Xuemin Liu:** Formal analysis. **Shaodong Zhou:** Formal analysis, Supervision, Conceptualization.

Declaration of Competing Interest

The authors declare that they have no known competing financial interests or personal relationships that could have appeared to influence the work reported in this paper.

Acknowledgements

The authors are grateful for the financial support from the National Natural Science Foundation of China (22078130, 21878265 and 21606104). We also appreciate the support for aggregate characterization from the Central Laboratory of School of Chemical and Material Engineering of Jiangnan University.

Appendix A. Supplementary material

Supplementary data to this article can be found online at https://doi.org/10.1016/j.molliq.2021.117464.

References

[1] J.J. Petkowski, W. Bains, S. Seager, J. Nat. Prod. 81 (2018) 423–446.
[2] R. Rino, C. Antonio, L.R. Giuseppe, D.M. Gabriella, P. Francesco, L. Antonio, N. Ettore, B. Alberto, C. Chiara, S. Anna, J. Med. Chem. 49 (2006) 3172–3184.
[3] I. Hussain, M.A. Yawer, M. Lalk, U. Lindequist, A. Villinger, C. Fischer, P. Langer, Bioorg. Med. Chem. 16 (2008) 9898–9903.
[4] U.K. Bandarage, T. Wang, J.H. Come, E. Perola, Y. Wei, B.G. Rao, Bioorg. Med. Chem. Lett. 18 (2008) 44–48.
[5] A. Kar, I.A. Sayyed, W.F. Lo, H.M. Kaiser, M. Beller, M.K. Tse, Org. Lett. 9 (2007) 3405–3408.
[6] B.T.V. Srinivas, V.S. Rawat, K. Konda, B. Sreedhar, Adv. Synth. Catal. 356 (2014) 805–817.
[7] M. Yang, H.Y. Shen, Y.Y. Li, C. Shen, P.F. Zhang, RSC Adv. 4 (2014) 26295–26300.
[8] X. Ge, F. Sun, X. Liu, X. Chen, C. Qian, S. Zhou, Mol Catal 449 (2018) 72–78.
[9] C. Shen, J. Xu, W. Yu, P. Zhang, Green Chem. 16 (2014) 3007–3012.
[10] G. La Sorella, G. Strukul, A. Scarso, Green Chem. 17 (2015) 644–683.
[11] T. Shen, S. Zhou, J. Ruan, X. Chen, X. Liu, X. Ge, C. Qian, Adv. Colloid Interfac 287 (2021) 102299.
[12] P. Sar, B. Saha, Adv. Colloid Interfac 284 (2020).
[13] G.N. Li, B. Wang, D.E. Resasco, ACS Catal. 10 (2020) 1294–1309.
[14] B.H. Lipshutz, Curr. Opin. Green Sustain. 11 (2018) 1–8.
[15] H. Firouzabadi, N. Iranpoor, A.A. Jafari, Adv. Synth. Catal. 347 (2005) 655–661.
[16] K.R. Reddy, K.C. Rajanna, K. Uppalaiah, Tetrahedron 54 (2013) 3431–3436.
[17] T. Nishikata, A.R. Abela, B.H. Lipshutz, Angew. Chem. Int. Ed. 49 (2010) 781–784.
[18] A. Kumar, M.K. Gupta, M. Kumar, Tetrahedron Lett. 51 (2010) 1582–1584.
[19] Z. Xu, T. Yang, X. Lin, J.D. Elliott, F. Ren, Tetrahedron Lett. 56 (2015) 475–477.
[20] B.H. Lipshutz, T.B. Petersen, A.R. Abela, Org. Lett. 10 (2008) 1333–1336.
[21] B.H. Lipshutz, G.T. Aguinaldo, S. Ghorai, K. Voigtritter, Org. Lett. 10 (2008) 1325–1328.
[22] Y. Zhang, B.S. Takale, F. Gallou, J. Reilly, B.H. Lipshutz, Chem. Sci. 10 (2019) 10556–10561.
[23] B. Jin, F. Gallou, J. Reilly, B.H. Lipshutz, Chem. Sci. 10 (2019) 3481–3485.
[24] S. Handa, B. Jin, P.P. Bora, Y. Wang, X. Zhang, F. Gallou, J. Reilly, B.H. Lipshutz, ACS Catal. 9 (2019) 2423–2431.
[25] F. Gallou, N.A. Isley, A. Ganic, U. Onken, M. Parmentier, Green Chem. 18 (2016) 14–19.
[26] S. Handa, E.D. Slack, B.H. Lipshutz, Angew. Chem. Int. Ed. 54 (2015) (1998) 11994–12001.

[27] S. Handa, M.P. Andersson, F. Gallou, J. Reilly, B.H. Lipshutz, Angew. Chem. Int. Ed. 55 (2016) 4914–4918.
[28] P. Klumphu, B.H. Lipshutz, J. Org. Chem. 79 (2014) 888–900.
[29] B.S. Takale, R.R. Thakore, S. Handa, F. Gallou, J. Reilly, B.H. Lipshutz, Chem. Sci. 10 (2019) 8825–8831.
[30] U.T. Duong, A.B. Gade, S. Plummer, F. Gallou, S. Handa, ACS Catal. 9 (2019) 10963–10970.
[31] T.N. Ansari, A. Taussat, A.H. Clark, M. Nachtegaal, S. Plummer, F. Gallou, S. Handa, ACS Catal. 9 (2019) 10389–10397.
[32] J.D. Smith, T.N. Ansari, M.P. Andersson, D. Yadagiri, F. Ibrahim, S. Liang, G.B. Hammond, F. Gallou, S. Handa, Green Chem. 20 (2018) 1784–1790.
[33] J. Brals, J.D. Smith, F. Ibrahim, F. Gallou, S. Handa, ACS Catal. 7 (2017) 7245–7250.
[34] N. Krause, Curr. Opin Green Sustain. 7 (2017) 18–22.
[35] A. Sanzone, S. Mattiello, G.M. Garavaglia, A.M. Calascibetta, C. Ceriani, M. Sassi, L. Beverina, Green Chem. 21 (2019) 4400–4405.
[36] B.H. Lipshutz, F. Gallou, S. Handa, ACS Sustain. Chem. Eng. 4 (2016) 5838–5849.
[37] J.E. Klijn, J. Engberts, J. Am. Chem. Soc. 125 (2003) 1825–1833.
[38] X. Ji, M. Tian, Y. Wang, Langmuir 32 (2016) 972–981.
[39] J.E. Klijn, J. Engberts, Langmuir 21 (2005) 9809–9817.
[40] M. Akbarzadeh, Z. Moosavi-Movahedi, A. Shockravi, R. Jafari, K. Nazari, N. Sheibani, A.A. Moosavi-Movahedi, J. Mol. Catal. A-Chem. 424 (2016) 181–193.
[41] G. Hamasaka, T. Muto, Y. Uozumi, Angew. Chem. Int. Ed. 50 (2011) 4876–4878.
[42] N. Kaur, S. Kaur, G. Kaur, A. Bhalla, S. Srinivasan, G.R. Chaudhary, J. Mater. Chem. A 7 (2019) 17306–17314.
[43] X. Liu, J. Wang, Z. Cui, H. Yao, X. Ge, W. Chen, F. Sun, RSC Adv. 7 (2017) 26440–26445.
[44] X. Ge, S. Zhang, X. Chen, X. Liu, C. Qian, Green Chem. 21 (2019) 2771–2776.
[45] N. Drillaud, E. Banaszak-Leonard, I. Pezron, C. Len, J. Org. Chem. 77 (2012) 9553–9561.
[46] U. Komorek, K.A. Wilk, J Colloid Interf Sci 271 (2004) 206–211.
[47] M.J.L. Castro, A.F. Cirelli, J. Kovensky, J. Surfactants Deterg. 9 (2006) 279–286.
[48] K.A. Wilk, L. Syper, B. Burczyk, I. Maliszewska, M. Jon, B.W. Domagalska, J. Surfactants Deterg. 4 (2001) 155–161.
[49] F.M. Menger, B.N.A. Mbadugha, J. Am. Chem. Soc. 123 (2001) 875–885.
[50] K.A. Wilk, L. Syper, B. Burczyk, A. Sokolowski, B.W. Domagalska, J. Surfactants Deterg. 3 (2000) 185–192.
[51] T. Yoshimura, K. Ishihara, K. Esumi, Langmuir 21 (2005) 10409–10415.
[52] K. Sakai, S. Umezawa, M. Tamura, Y. Takamatsu, K. Tsuchiya, K. Torigoe, T. Ohkubo, T. Yoshimura, K. Esumi, H. Sakai, M. Abe, J. Colloid Interf Sci. 318 (2008) 440–448.
[53] T. Yoshimura, S. Umezawa, A. Fujino, K. Torigoe, K. Sakai, H. Sakai, M. Abe, K. Esumi, J. Oleo Sci. 62 (2013) 353–362.
[54] U. Laska, K.A. Wilk, I. Maliszewska, L. Syper, J. Surfactants Deterg. 9 (2006) 115–124.
[55] M. Johnsson, A. Wagenaar, J. Engberts, J. Am. Chem. Soc. 125 (2003) 757–760.
[56] M. Scarzello, J.E. Klijn, A. Wagenaar, M.C.A. Stuart, R. Hulst, J. Engberts, Langmuir 22 (2006) 2558–2568.
[57] S. Warwel, F. Bruse, H. Schier, J. Surfactants Deterg. 7 (2004) 181–186.
[58] S. Warwel, F. Bruse, J. Surfactants Deterg. 7 (2004) 187–193.
[59] Z. Xin, B. Du, S. Yan, S. Du, J. Ding, Z. Yang, W. Ren, J. Biomater. Sci.-Polym. Ed. 25 (2014) 1045–1061.
[60] M.J.L. Castro, J. Kovensky, A.F. Cirelli, Tetrahedron Lett. 38 (1997) 3995–3998.
[61] K.A. Wilk, L. Syper, B.W. Domagalska, U. Komorek, I. Maliszewska, R. Gancarz, J. Surfactants Deterg. 5 (2002) 235–244.
[62] J. Eastoe, P. Rogueda, A.M. Howe, A.R. Pitt, R.K. Heenan, Langmuir 12 (1996) 2701–2705.
[63] X.M. Liu, X. Liao, S.H. Zhang, S. Chang, L. Cheng, M. Ge, X. Ge, J. Chem. Eng. Data 64 (2019) 60–68.
[64] D.R. Perinelli, M. Cespi, N. Lorusso, G.F. Palmieri, G. Bonacucina, P. Blasi, Langmuir 36 (2020) 5745–5753.
[65] A. Chen, X. Liu, Y. Wu, G. Luo, J.-H. Xu, Langmuir 36 (2020) 4600–4606.
[66] S. Deodhar, P. Rohilla, M. Manivannan, S.P. Thampi, M.G. Basavaraj, Langmuir : the ACS journal of surfaces and colloids 36 (2020) 8100–8110.
[67] S. Kumar, A. Damyanti Sharma, Kabiruddin, Langmuir 19 (2003) 3539-3541.
[68] T.M. Mccoy, J.B. Marlow, A.J. Armstrong, A.J. Clulow, C.J. Garvey, M. Manohar, T. A. Darwish, B.J. Boyd, A.F. Routh, R.F. Tabor, Biomacromolecules 21 (2020) 4569–4576.
[69] C. Bannwarth, S. Ehlert, S. Grimme, J. Chem. Theory Comput. 15 (2019) 1652–1671.
[70] C. Adamo, V. Barone, J. Chem. Phys. 110 (1999) 6158–6170.
[71] F. Weigend, R. Ahlrichs, Phys. Chem. Chem. Phys. 7 (2005) 3297–3305.
[72] Gaussian 16, Revision A.03, M. J. Frisch, G. W. Trucks, H. B. Schlegel, G. E. Scuseria, M. A. Robb, J. R. Cheeseman, G. Scalmani, V. Barone, G. A. Petersson, H. Nakatsuji, X. Li, M. Caricato, A. V. Marenich, J. Bloino, B. G. Janesko, R. Gomperts, B. Mennucci, H. P. Hratchian, J. V. Ortiz, A. F. Izmaylov, J. L. Sonnenberg, D. Williams-Young, F. Ding, F. Lipparini, F. Egidi, J. Goings, B. Peng, A. Petrone, T. Henderson, D. Ranasinghe, V. G. Zakrzewski, J. Gao, N. Rega, G. Zheng, W. Liang, M. Hada, M. Ehara, K. Toyota, R. Fukuda, J. Hasegawa, M. Ishida, T. Nakajima, Y. Honda, O. Kitao, H. Nakai, T. Vreven, K. Throssell, J. A. Montgomery, Jr., J. E. Peralta, F. Ogliaro, M. J. Bearpark, J. J. Heyd, E. N. Brothers, K. N. Kudin, V. N. Staroverov, T. A. Keith, R. Kobayashi, J. Normand, K. Raghavachari, A. P. Rendell, J. C. Burant, S. S. Iyengar, J. Tomasi, M. Cossi, J. M. Millam, M. Klene, C. Adamo, R. Cammi, J. W. Ochterski, R. L. Martin, K. Morokuma, O. Farkas, J. B. Foresman, and D. J. Fox, Gaussian, Inc., Wallingford CT, 2016.
[73] T. Lu, F.W. Chen, J. Comput. Chem. 33 (2012) 580–592.
[74] W. Humphrey, A. Dalke, K. Schulten, J. Mol. Graph. Model. 14 (1996) 33–38.